Current Optics and Photonics

MS ID: 230165

Manuscript Type: Invited Review Paper

Title: Review on Metasurfaces with Extraordinary Flat-optic Functionalities

Keywords: Metasurface, Pancharatnam-Berry phase, Nanophotonics, Flat-optics, Nanoantennas

Abstract:
This paper presents a comprehensive review on metasurface technology, focused on its significant role in extraordinary flat-optic functionalities. Traditional optical components, though optimized, are bulky and less congruent with modern integrated electromagnetic and photonic systems. Metasurfaces, recognized as the 2D counterparts of bulk metamaterials, offer solutions with their planar, ultra-thin, and lightweight structures. Their meta-atoms are adept at introducing abrupt shifts in optical properties, paving the way for high precision light manipulation. By introducing the key design principles of these meta-atoms, such as the magnetic-dipole and Pancharatnam-Berry phase, various application in wavefront shaping and beam forming via simple amplitude/phase manipulation to advanced applications including retroreflectors, and Janus metasurfaces, multiplexing of optical wavefronts, data encryption, and metasurfaces for quantum applications are reviewed.

Vol. *, No. *, Month Year, pp. *–*

Current Optics and Photonics

Regular Paper

Review on Metasurfaces with Extraordinary Flat-optic Functionalities

Hee-Dong Jeong[1], Sang-Woo Shin[1], Hyuntai Kim[2], and Seung-Yeol Lee[1]*

School of Electronic and Electrical Engineering, Kyungpook National University, Daegu 41566, Korea

Department of Electronic and Electrical Converged Engineering, Hongik University, Sejong, 30016, Korea

** Corresponding author: seungyeol@knu.ac.kr*

ORCID 0000-0002-8987-9749

Abstract:
This paper presents a comprehensive review on metasurface technology, focused on its significant role in extraordinary flat-optic functionalities. Traditional optical components, though optimized, are bulky and less congruent with modern integrated electromagnetic and photonic systems. Metasurfaces, recognized as the 2D counterparts of bulk metamaterials, offer solutions with their planar, ultra-thin, and lightweight structures. Their meta-atoms are adept at introducing abrupt shifts in optical properties, paving the way for high precision light manipulation. By introducing the key design principles of these meta-atoms, such as the magnetic-dipole and Pancharatnam–Berry phase, various application in wavefront shaping and beam forming via simple amplitude/phase manipulation to advanced applications including retroreflectors, and Janus metasurfaces, multiplexing of optical wavefronts, data encryption, and metasurfaces for quantum applications are reviewed.

Keywords: Metasurface, Pancharatnam–Berry phase, Nanophotonics, Flat-optics, Nanoantennas
OCIS codes: (160.3918) Metamaterials; (160.4236) Nanomaterials; (310.6628) Subwavelength structures, nanostructures; (230.0230) Optical devices; (240.6680) Surface plasmons;

*Corresponding author: seungyeol@knu.ac.kr, ORCID 0000-0002-8987-9749

Color versions of one or more of the figures in this paper are available online.

I. INTRODUCTION

The precise manipulation of light, a cornerstone of various applications such as optical sensing, imaging, and communication, is generally based on the alteration of amplitude, phase, and polarization states of light, which ultimately induce a desired outcoming light such as beam steering or wavefront shaping [1–3]. Traditionally, these tasks have been accomplished via bulk optical components based on refraction, reflection, absorption, and/or diffraction of light. Despite their optimized performance and prevalence, these traditional tools have fundamental limitations due to their bulkiness and heaviness, which make them less suited for the modern electromagnetic and photonic systems, where integration and miniaturization are essential [4, 5].

The solution to these challenges has emerged in the form of metasurfaces, a single-layer or few-layer stacks of planar structures, which can be readily fabricated using existing technologies such as lithography and nano-imprinting [6–10]. As the two-dimensional (2D) equivalents of bulk metamaterials, the meta-atoms of metasurfaces designed to have their own functionality to introduce abrupt changes in optical properties [11–14]. The rapid advances in metasurfaces have facilitated an era of flat-optics, characterized by ultra-thin, lightweight, and planar devices capable of manipulating light with high precision and efficiency.

In this review, we would like to provide a summary and perspective by examining the recent advancements in metasurface technology especially focused on their extraordinary functionality. Beginning with the explanation of frequently-used design principles of meta-atoms such as electromagnetic phenomena including magnetic-dipole, Pancharatnam–Berry (PB) phase, as well as their use in wavefront shaping and beam forming applications such as meta-lens and metasurface hologram techniques will be introduced. The functionality of metasurfaces can be numerously designed based on the feature of their meta-atom, or a subgroup of meta-atoms functions like super-pixel, which leads to induce the various features such as phase gradient designer plate, retroreflector, optical Janus metasurfaces, polarization conversion, nonlinear optical phenomena, single-photon manipulation, and pulse reshaping.

In section 2, we would like to briefly review the basic principles that frequently used for designing meta-atoms. After that, we would like to focus on various applications of metasurfaces classified with its features and functionality. Starting from simple amplitude/phase manipulation, various extraordinary features of metasurfaces such as multiplexing of optical wavefronts, data encryption, asymmetric transmission and Janus metasurfaces, and some quantum applications based on metasurface design will be reviewed.

II. BASIC PRINCIPLE OF META-ATOMS

The performance of the phase-gradient characteristics of given metasurface is often verified by providing anomalous reflection and refraction, or designing lens function phase profile to provide a meta-lens geometry. After the addition of gradient phase profile caused by metasurface into Snell's law, often called *generalized Snell's law* which includes the out of the plane reflection and refraction component can be expressed as [15, 16],

$$\begin{cases} \sin\boldsymbol{\theta}_r - \sin\boldsymbol{\theta}_i = \frac{1}{n_i k_0}\frac{d\Phi}{dx} \\ \cos\boldsymbol{\theta}_r \sin\boldsymbol{\varphi}_r = \frac{1}{n_i k_0}\frac{d\Phi}{dy} \end{cases}, \quad (1)$$

$$\begin{cases} n_t \sin\theta_t - n_i \sin\theta_i = \frac{1}{k_0}\frac{d\Phi}{dx} \\ \cos\theta_t \sin\varphi_t = \frac{1}{n_t k_0}\frac{d\Phi}{dy} \end{cases}. \quad (2)$$

Here, we assume the case that *xz plane* is the plane of incidence, and *y-axis* is perpendicular to the plane of incidence. $\mathbf{n}_i, \mathbf{n}_t$ are refractive indexes for incident and refracted region. Angle parameters $\boldsymbol{\theta}_i, \boldsymbol{\theta}_r$ and $\boldsymbol{\theta}_t$ indicates the in-plane angles of incident, reflected, and refracted light at the metasurface, whereas $\boldsymbol{\varphi}_r$ and $\boldsymbol{\varphi}_t$ are out-of-plane angle from plane of incidence for reflected and refracted light, respectively. In addition, $\boldsymbol{\Phi}$ indicates the phase gradient artificially made by the metasurface.

Using generalized Snell's law, it is considered that the reflected and refracted angle of incident light can be arbitrary tuned by the metasurface. Experimental demonstration of these phase gradient metasurface can be achieved by various type of meta-atoms, which will be followed in the next few sections.

2.1. Plasmonic resonances of metallic nanostructure

Since the field of metasurface have been tightly related to that of bulk metamaterials, the pioneering works of metasurface design principle have been frequently used metallic nanostructures as their meta-atom and utilize plasmonic resonances. The wavefront shaping with metasurfaces has been shown as the first meta-atom offering full phase control of light from 0 to 2π, with the V-shaped antenna [15]. Carefully designed symmetric and anti-symmetric plasmonic resonance are hybridized, to produce strong phase modulation of cross-polarized scattered light from the meta-atoms. Through comprehensive parametric study of given meta-atom geometry, a phase-gradient metasurface has been reported by changing the length and the orientation angle of the V-shaped nanoantenna, which is working on mid-infrared region is shown in Fig. 1(a).

Moreover, such phase-gradient characteristics of plasmonic nano-antenna can be achieved with various geometries, including C-shaped resonator [17, 18], mirror-imaged dipole antenna [19], and nanoapertures [20–22].

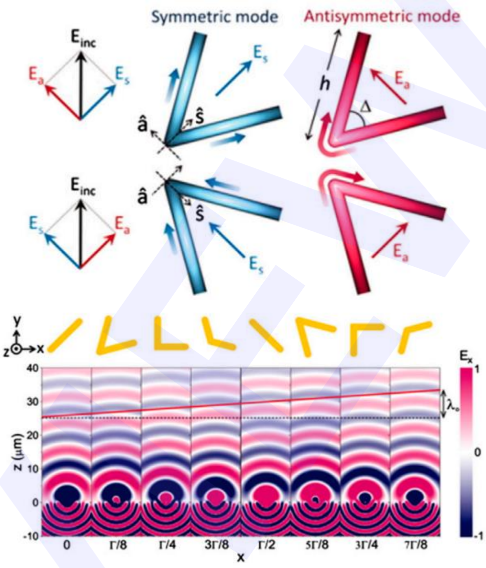

(a)

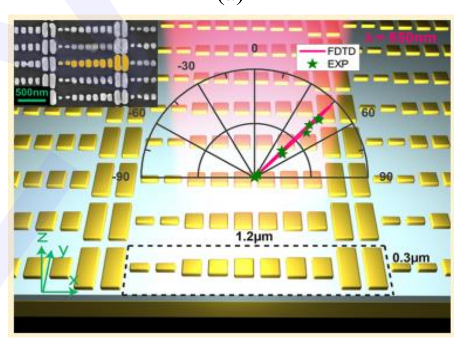

(b)

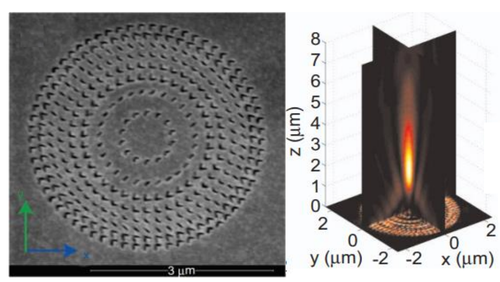

(c)

FIG. 1. Meta-atoms based on plasmonic resonances. (a) Design principle and phase characteristics of V-shaped gold optical antennas offering full phase control of light from 0 to 2π. (b) Reflection-type metasurface that uses dipole antenna resonance on metal-mirror. (c) Babinet-inverted nano-antennas as a meta-atom to provide ultra-thin, compact meta-lense.

Reprinted with permission from [15], [19], and [20].

2.2. Pancharatnam-Berry phase

Although plasmonic nanoantennas successfully demonstrate the phase-gradient metasurfaces at mid-infrared and near-infrared range, resonant characteristics of nanoantenna often restrict the operation bandwidth within a certain range and high thermal loss of metallic geometry may reduce the overall performance especially for transmission type phase-gradient metasurfaces [23].

One of the solutions to overcome abovementioned issues is applying Pancharatnam–Berry phase into metasurface [24, 25]. PB-phase, or often referred as geometric phase, have known as a strong and intuitive method to modulate the phase of the circularly polarized light during the transmission of meta-atom. When designing the metasurface, PB-phase often demonstrated by rotation of meta-atom as shown in Fig. 2(a). Using the Jones matrix form, phase retardation caused by rotated meta-atom can be expressed as [26, 27],

$$\boldsymbol{\mathcal{J}} = \begin{bmatrix} \boldsymbol{t_{\mathrm{u}}\cos^2\varphi + t_{\mathrm{v}}\sin^2\varphi} & \boldsymbol{(t_{\mathrm{u}} - t_{\mathrm{v}})\sin 2\varphi/2} \\ \boldsymbol{(t_{\mathrm{u}} - t_{\mathrm{v}})\sin 2\varphi/2} & \boldsymbol{t_{\mathrm{u}}\sin^2\varphi + t_{\mathrm{v}}\cos^2\varphi} \end{bmatrix} \tag{3}$$

In this equation, $\boldsymbol{t_{\mathrm{u}}}$, $\boldsymbol{t_{\mathrm{v}}}$ indicates the transmission coefficients of anisotropic meta-atom along its principle axes, and $\boldsymbol{\varphi}$ indicates the angle between global axes (x, y) and local axes of meta-atom (u, v). If we assume the circular polarization incidence, the Jone vector form of transmitted light which have spin state of $\boldsymbol{\sigma}$ can be written as,

$$\boldsymbol{\mathcal{J}}\frac{1}{\sqrt{2}}\begin{bmatrix}\boldsymbol{1}\\ \boldsymbol{j\sigma}\end{bmatrix} = \frac{1}{2}\left[(\boldsymbol{t_{\mathrm{u}}}+\boldsymbol{t_{\mathrm{v}}})\begin{bmatrix}\boldsymbol{1}\\ \boldsymbol{j\sigma}\end{bmatrix} + (\boldsymbol{t_{\mathrm{u}}}-\boldsymbol{t_{\mathrm{v}}})\,\mathbf{exp}(\boldsymbol{j2\sigma\varphi})\begin{bmatrix}\boldsymbol{1}\\ \boldsymbol{-j\sigma}\end{bmatrix}\right] \tag{4}$$

which means that the cross-polarization phase component of transmitted light is delayed by the twice of the orientation angle of meta-atom ($\mathbf{exp}(\boldsymbol{j2\sigma\varphi})$), whereas co-polarized light does not affected by the orientation angle.

According to Eq. (4), it is notable that it is possible to perfectly remove the co-polarization component by of scattered light from the meta-atom by precisely designing the $\boldsymbol{t_{\mathrm{u}}}$ and $\boldsymbol{t_{\mathrm{v}}}$ to have π-phase difference like half wave retarder. Moreover, since the Eq. (4) is not directly affected by the wavelength, metasurface using PB-phase is quite suitable for designing broadband, highly-efficient transmitted type phase gradient metasurfaces, therefore the principle has been widely applied to various metalens and meta-holograms [28, 29] as shown in Fig. 2(b).

2.3. Polarization-independent propagation phase

Since phase retardation caused by the PB-phase only affected to the cross-polarization component of incident circular polarization, most of applications that uses PB-phase has polarization sensitive characteristics. For polarization insensitive applications, propagation phase or detour phase retardations are often applied, or simultaneously applied to provide more degree of freedom in metasurface [30, 31].

As shown in Fig. 2(c), the tuning of phase retardation for polarization insensitive metasurface uses isotropic meta-atom such as cylinder or square nanopillars. Here, the size of meta-atom may affect to the variation of effective refractive index of guided mode through the meta-atoms. Therefore, these type of meta-atoms generally have higher aspect-ratio than meta-atoms based on plasmonic resonance or PB-phase, therefore materials of high-refractive index such as TiO_2 are often used to improve the effect of meta-atom size variation. Another example of polarization independent phase retardation is applying detour phase, which often indicates the relative phase difference caused by spatial displacement of meta-atom scatterer itself, which can be either longitudinal or transverse to the incident wave. However, the limitation of detour-phase is that the amount of phase delay is significantly altered by operating wavelength, because it is determined by the ratio of spatial displacement and the wavelength, which has a limitation to use for broadband operation of metasurface.

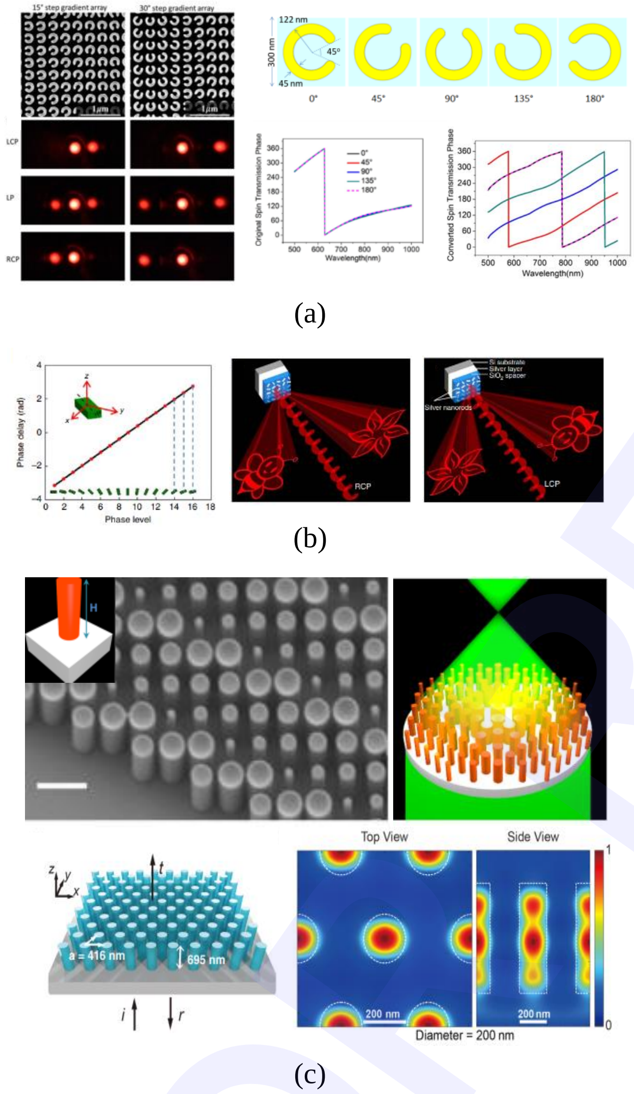

FIG. 2. (a) Meta-atom that used Pancharatnam-Berry phase with split-ring antenna array for beam steering. (b) Meta-hologram with helicity multiplexed images based on Pancharatnam-Berry phase. (c) Examples of polarization insensitive metasurface based on isotropic meta-atoms Reprinted with permission from [27], [28], [30] and [31].

III. METASURFACES WITH EXTRAORDINARY FUNCTIONALITIES

In recent research, the phase delay mechanisms explained in chapter 2 does not only solely applied but also adapted together for increasing the degree of freedom for designing the novel functionalities of meta-atoms. Such functionalities can be used for multiplexing the phase information [32, 33], or more precise control of transmitted light which can simultaneously control the complex amplitude and polarization states [34, 35], displaying 2D/3D image together [36], and other applications. This chapter will review the recent progress of metasurface applications that provide extraordinary functionalities with appropriate categorization.

3.1. Metasurface for next-generation display applications

Based on the design principles of meta-atoms explained in the previous section, one of the most promising applications for metasurface operating in visible range is replacing various optical components of display for more compactness and better efficiency. Because of the usefulness of metasurface in phase control, shaping and designing digital hologram has been frequently researched and often integrated with cavity structure for color selectively [37, 38]. As shown in Fig. 3(a), the work done by Y. Hu et. al. show integration of polarization independent metasurface into monolithic Fabry–Pérot (FP) cavity which is acts as a RGB color-filter, in order to achieve low-crosstalk and high-efficiency. 3D integration of metasurfaces by these two structures provides a function of microprints enabled by a monolithic colour filter microarray as well as hologram generation. Microprint image simultaneously observed when the device is illuminated by white light, while a full-colour hologram image can be projected under full color laser illumination [39].

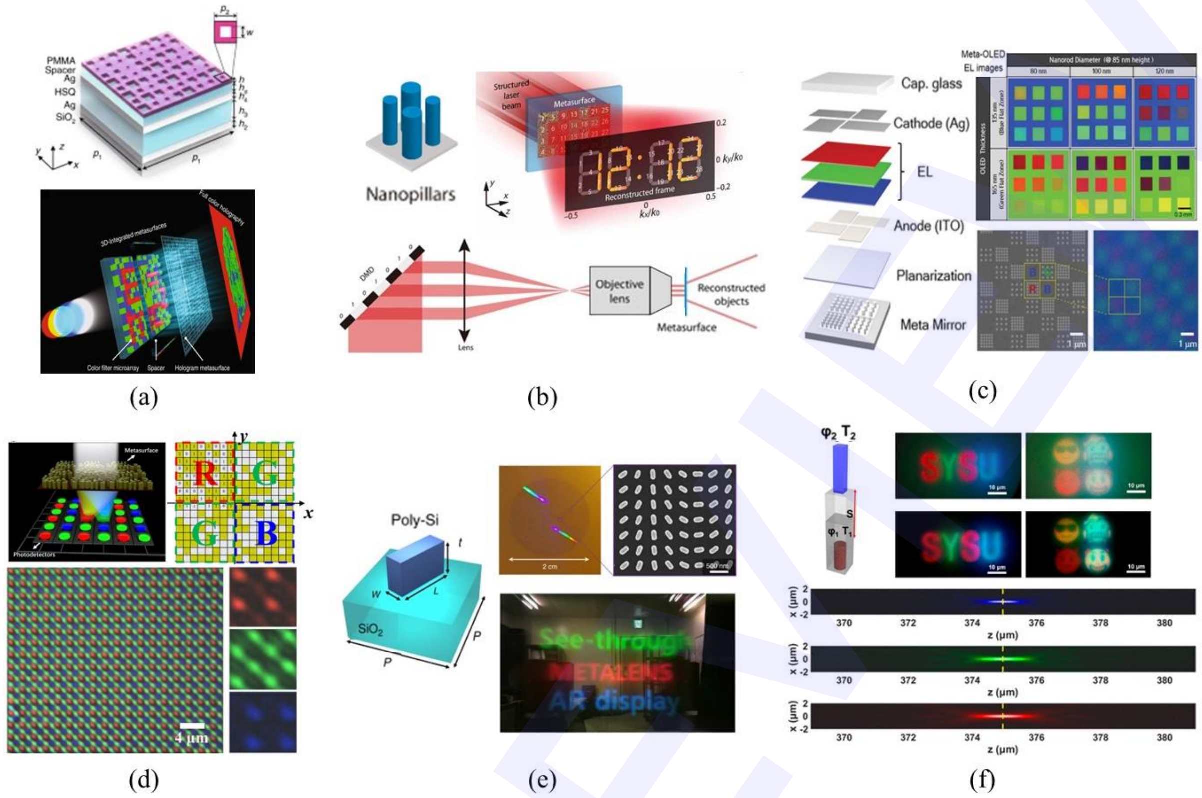

FIG. 3. Metasurfaces for various display applications. (a) Integration of micro-cavity color filter with metasurface for low-crostalk, full-color holography. (b) Dynamic meta-holography using space channel switching operation. (c) Replacement of fine metal mask into metasurface mirror for micro-OLED. (d) Pixel-level color routing metasurface for image sensor. (e) Using metalens as a polarization-selective lens for augmented reality. (f) Achromatic metalens doublet for digital imaging. Reprinted with permission from [39–43] and [45].

One of the advantages of using metasurface for digital hologram application is laid on its tiny pixel pitch, which enables hologram generation within very small region with sufficiently high beam steering angle. The work shown in Fig. 3(b) successfully applied such advantage by introducing space channel meta-hologram, which used similar approach of 7-segment system in electronic circuit [40]. The whole metasurface is divided into several spatial subsections consists of silicon nitride nanopillars, and each of subsection provide a segmented message as a hologram. Each of spatial channel can be illuminated separately by using digital multimirror device (DMD), therefore it can support dynamic hologram message with high frame rate (9523 frame per second) has been achieved.

Obviously, the light manipulation characteristics of metasurfaces are not restricted to hologram applications; they can also be applied to more practical display devices such as micro-OLEDs. As illustrated in Fig. 3(c), the work done by Joo et al. incorporated a nanopillar-type metasurface into the bottom mirror of a micro-OLED device [41]. The phase retardation from the metasurface is optimized to produce the appropriate resonance shift of the micro-OLED Fabry–Pérot cavity. This cavity is initially designed for a blue pixel but is altered to the cavity condition of a red or green pixel due to the resonance shift. Using this method, it is possible to replace the fine-metal mask

(FMM) for RGB subpixels, which presents practical challenges for achieving higher-resolution OLED displays.

Like these, metasurface can replace conventional optical elements by thinner, flatter, and even merging two functionalities of conventional optical element into single metasurface. The work introduced in Fig. 3(d) shows such example, which provides pixel-level color router that combines the functionalities of microlens array and bayer color filters, using the inverse design method of a genetic optimization, the proposed metasurface can also improve the efficiency about 84% at visible range, which can be applicable to span a white light into RGB colors and then focus each of them into different location within a single metasurface [42]. Therefore, the proposed work can be applicable to high-resolution CMOS image sensors, up to pixel-size of 1 μm by 1 μm scale.

Another well-known application of metasurface is using meta-lens as a polarization selective see-through display element for augmented reality display. As explained in chapter 2, PB-phase can produce phase retardation only for cross-polarization component, whereas co-polarization component does not affected. Therefore, metalens eyepiece combined with circular polarizer simultaneously show external environment and AR image which has been demonstrated by nano-imprinting technology. A prototype metalens for AR application have a lens aperture of 20 mm and a high NA of 0.61 for achieving a wide FOV, which is depicted in Fig. 3(e) [43].

The meta-lens is one of the most well-known and fascinating candidates of metasurface-based application that can be practically used. Among numerous research that design and fabricate the meta-lens [44], the work introduced in Fig. 3(f) applied doublet structure in meta-lens to design an achromatic characteristic in meta-lens. Unlike previously reported PB-phase based achromatic meta-lens [45], given geometry has polarization-independent characteristic for broad range with high NA of 0.8 in visible range, which can be led to the applications of high-quality full-color hologram generation.

3.2. Multiplexing and Encrypting phase with metasurface

As we explained in section 2, there are various methods to generate abrupt phase retardation such as PB-phase, detour phase, and guided modal phase, and these principles can be merged to provide more degree of freedom in metasurface design. Such degree of freedom used to not only control the transmitted/reflected light with more precisely, but also for multiplexing phase information within single metasurface. For example, one of the pioneering works for multiplexing metasurface was achieved by mixing the PB-phase with guided modal phase [46–48], which can produce two independent hologram images according to input polarization handedness [49–51]. Moreover, recently, researchers also developing a kind of metasurfaces that can express certain information either actively or passively, such characteristics can be achieved various routes by merging various principles of metasurface design in a single metasurface. This section will briefly review some of these works.

Based on the polarization-selective multiplexing characteristics of metasurface, metasurface integrated with liquid-crystal can be one of the simplest but the most practical use of tunable optical phase generation [52, 53]. As shown in Fig. 4(a), polarization-multiplexed achromatic dielectric metalens, which is designed with meta-atoms of anisotropic retarded phase properties, is integrated with twisted nematic liquid crystals to demonstrate tunable focal length characteristics [52].

If the optical phase information is only multiplexed through certain polarization channel, the maximum number of multiplexed data might be significantly restricted. To increase the number of multiplexed data, either optical angular momentum [54] or vectorial hologram [55] can be used. The work proposed via vectorial hologram is shown in Fig 4(b), to produce nine

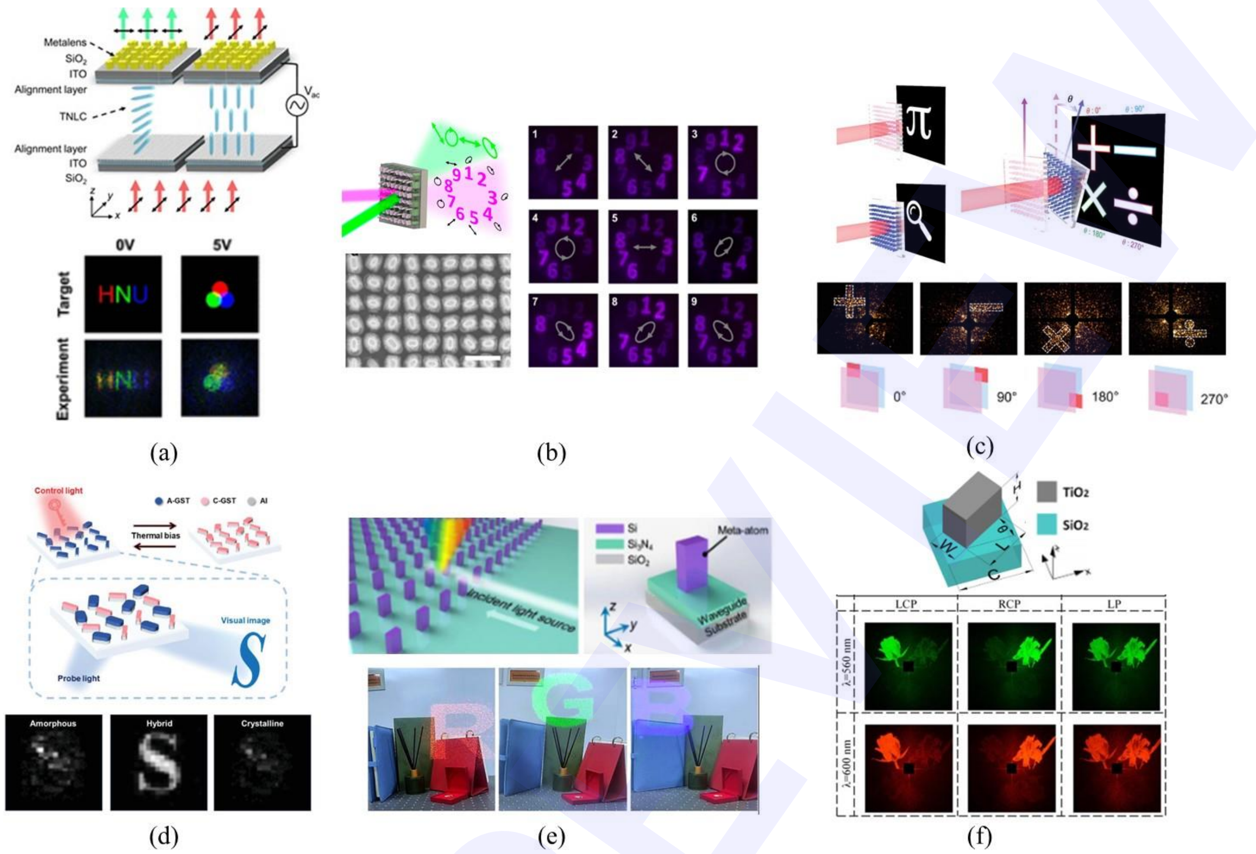

FIG. 4. Metasurfaces for multiplexing and encrypting optical information. (a) Tunable polarization-multiplexed metalens. (b) Optical encryption platform using vectorial hologram with multiple polarization channels. (c) Multiplexing hologram information with cascaded metasurfaces. (d) Temperature-sensitive data encryption metasurface using thermally-driven phase change material rods. (e) Multiplexing full-color RGB information via single metasurface through on-chip waveguide modes and PB-phase. (f) Three-channel metasurface that simultaneously show nanoimprinting image and two holographic images. Reprinted with permission from [52], [55], [56], [61], [62] and [63].

explicit information, authors design a superpixel consists of nine types of subpixels, which is designed to reconstruct certain holographic image with properly designed polarization state, and randomly place for suppression of grating effect. Each of subpixel consists of two type of groups that produce opposite type of PB-phase.

Recent advance in optimizing techniques such as gradient optimizer lead to the development of novel type of metasurfaces that can produce unique functionalities [56]. The work presented in Fig. 4(c) shows that cascade alignment of two metasurface can be used to give a new degree of freedom to design optical phase information. Based on the phase profile optimizer based on gradient descent algorithm, the cascaded metasurface reconstructs four types of different images according to the orientation angle between two metasurfaces, as well as each of metasurface provide its own hologram images by tracking and updating the gradient of total mean square error calculated from the optimizer.

For active metasurface, phase change materials working on visible or infrared range such as $Ge_2Sb_2Te_5$ or VO_2 have been applied in numerous works [57–60]. Among them, the works shown in Fig. 4(d) provide a unique route to temperature-sensitive data encryption in active metasurface [61]. Two-type of $Ge_2Sb_2Te_5$ nanorods, which have different phase-change temperatures because of the different size, can be used to hide the hologram image data which can only be observed at a very narrow region of temperature condition. Although the proposed work only used two types of nanorod and a single type of phase change materials, the given principle has more potential to express multi-level information by applying various sizes of meta-atoms or adding other phase change materials simultaneously.

Multiplexing of hologram can also be conducted by illumination directions and method, one of the recent representative example is shown in Fig. 4(e) [62]. In this work, the meta-atoms are simple rectangular rod-type that produce PB-phase, which is designed for producing the hologram information (for red light) directly illuminate from the bottom of the metasurface. However, two more phase information (for green and blue lights) are integrated into the metasurface by applying detour phase along horizontal and vertical directions, and the input signals are provided through the waveguide mode within the metasurface plate. Since these waveguide modes are often used in recent AR applications the given metasurface has a great potential to multiplexing full-colored images without using multiple number of waveguides. Another example of data multiplexing with metasurface is shown in Fig. 4(f), which can simultaneously show three channel of multiplexed images consists of one 2D micro-image and two far-field holographic image, respectively [63].

3.3. Asymmetric transmission and Janus metasurfaces

Optical Janus effect, inspired by a Roman god who has two different faces, often indicates the optical phenomenon which displays different information according to the observation side. The phenomenon has been classified to asymmetric reflection and transmission, the asymmetric reflection has been simply demonstrated without applying meta-atom because the reflection coefficients can be different without chiral geometry. Therefore, a simple nanoparticle deposition on asymmetric material interface can lead to the optical Janus reflection [64], and by applying liquid permeable random nano-island FP etalon, such Janus reflection has been applied to optical camouflage applications as shown in Fig. 5(a) [65]. In this work, it has been shown that the optical camouflage condition, which means that overall reflection spectra of liquid-sensitive region is matched to nearby reference region, can be accompanied with optical Janus effect. On the other hand, the asymmetric transmission often requires more complicate meta-atom geometry such as cascade stacking of metasurfaces or chiral meta-atoms [66, 67]. Recently, the work done by K. Chen et. al. provide an directional Janus metasurface which can display two different holographic information from metasurface plate composed of cascaded subwavelength scale impedence sheet as shown in Fig. 5(b). Using the rotatory alignment of meta-atoms, authors analytically derive the unidirectional features on their metasurfaces, and by distributing two types of meta-atoms that provide phase gradient characteristic for forward (or backward) direction but totally blocking their transmission for backward (or forward) direction, it was possible to independently design the phase gradient characteristics of given metasurface for forward and backward side illuminations of incident light, respectively.

Instead of using unidirectional light transmission and their spatial multiplexing for realizing optical Janus transmission, the work shown in Fig. 5(c) applied polarization multiplexing for optical Janus metasurface [68]. The cascaded layers of metallic nanorod, dielectric spacers, and metallic nanowire successfully designed to provide an unidirectional phase gradient

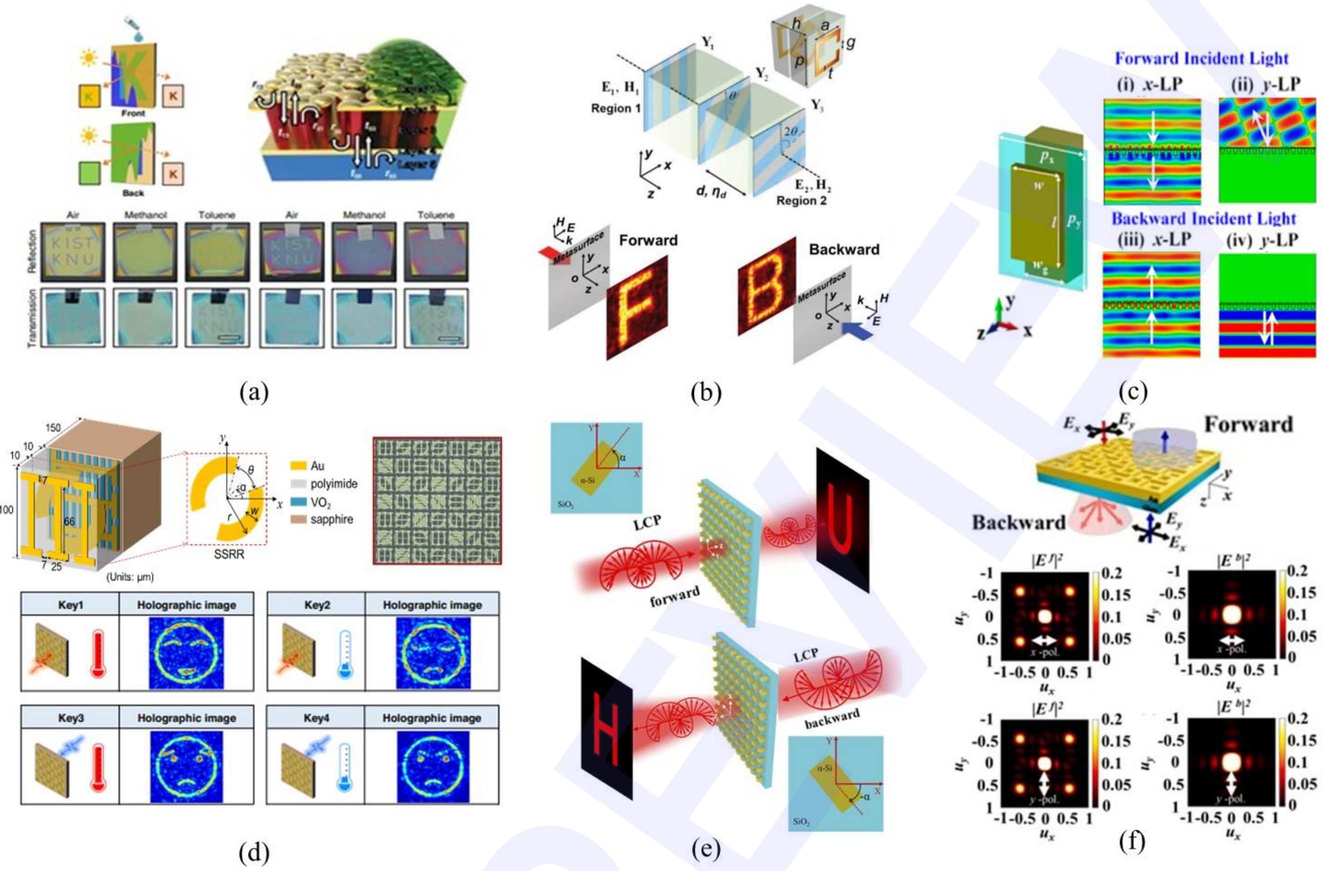

FIG. 5. Metasurfaces for asymmetric optical characteristics, i. e. Janus metasurface. (a) Asymmetric optical camouflage using FP cavity consists of random distributed metallic nano islands. (b) Directional Janus metasurface using cascaded subwavelength anisotropic impedance sheets. (c) Polarization-selective Janus metasurface composed of cascaded layers of metallic nanorod and nanowires. (d) Thermally active Janus metasurface for directional holography in terahertz region. (e) A single-layered Janus metasurface based of precise control of PB phase. (f) Polarization-independent diffractive Janus metasurface for asymmetric diffraction. Reprinted with permission from [65], [67], [68], [69], [70] and [72].

characteristics only available for certain linear polarization, whereas its orthogonal polarization is not affected by the phase gradient profile designed by the nanorods.

Since the Janus metasurface often requires complicate, cascaded, or chiral meta-atom geometry, it was not simple to apply active functionality into the Janus metasurface. However, recent work reported by B. Chen et. al. successfully demonstrated the active Janus metasurface working on the terahertz region as illustrated in Fig. 5(d) [69]. The tuning mechanism for active functionality is using VO_2 integrated meta-atom for thermally active impedance sheet. By conjunction with other cascaded metallic layers, authors proposed four independent phase informations in their work, which are tuned by illumination direction and thermal conditions, respectively.

Like these, metasurface with Janus functionalities has been greatly interested by many researchers. Some works are focused on multiplexing more information with more complex design of meta-atoms for further degree of freedom, whereas some others focused on to provide Janus functionality with simpler structures [70]. The work shown in Fig. 5(e) designs the Janus metasurface without using cascaded metasurface sheets. It is based on PB-phase therefore only working for circularly polarized light. By applying modified iterative algorithm to optimize the bi-directional hologram caused by opposite phase distribution caused by PB-phase, they successfully demonstrate the Janus hologram with a single-layer of metasurface plate. However, the limitation of the proposed work is that the metasurface should be working with certain circular polarization, and additional polarization filters should be placed to remove the co-polarized light from the PB-phase based metasurface.

In addition, the work shown in Fig. 5(f) also demonstrate the asymmetric metasurface with single-layered structure by using the mixed-cavity structure composed of single and double-step nanoapertures [71, 72]. In this work, the difference of effective periods observed by forward and backward side is a key feature for optical Janus characteristics. Here, the periodic arrangement of square shaped meta-atom enables the polarization-independent Janus functionality in its diffraction property. However, the proposed work was only limited to generate the diffracted beam, which does not show more complicate phase-gradient information such as meta-lens or meta-hologram.

3.4. Metasurfaces for photons and pulse manipulations

Recent great advances in metasurface technologies expand the use of metasurface from the conventional electromagnetic wave wavefront engineering to single-photon manipulation and pulse reshaping [73–76]. Figure 6 shows some of recent works that apply the metasurface into such photon-based or pulse-reshaping applications.

In the field of plasmonics, spiral-shaped gratings as shown in Fig. 6(a) often considered as a useful geometry for conversion of optical spin-state which are assisted by spin-angular momentum interactions during the surface plasmon polariton (SPP) coupling [77– 80]. The work shown in Fig. 6(a) demonstrate the generation of highly directional single-photon having certain spin-angular momentum state based on the SPP mode coupling from spiral-shaped metasurface composed of concentric periodic width-varying dielectric nanoridges [81]. Tightly focused pump beam illustrated as a green cones of Fig. 6(a) may produce a strong longitudinal electric field, which can activate the quantum emitter located at the center of metasurface, and finally guided to only produce certain spin-state of photon via SPP mode coupling into surrounding nanoridges.

Spontaneous parametric down-conversion (SPDC), known as a nonlinear phenomenon that converts one photon of higher energy into a pair of photons of lower energy, is often considered as an important process for generation of entangled photon pairs [82]. The work that described in Fig. 6(b) used nonlinear metasurface to strongly enhance the SPDC. The metasurface made by nonlinear material such as lithium niobate, to produce photon pair with the enhancement of 2 orders of magnitude compared to the unpatterned film of same thickness material. Metasurface structure used in this work composed on arrangement of nanoresonators in the shape of truncated pyramids, which can significantly enhance the electric field nearby the metasurface.

Various metasurfaces have been developed not only for generation and enhancement of entangled photons, but also has been applied to the detection of interfered photon states. The work shown in Fig. 6(c) demonstrate the interference of multiphoton state and their reconstruction with metasurface. It has been shown that the all-dielectric metasurface can be used to measure the correlation states of multiphoton density matrix without direct polarization measurement detection, by splitting the N-photon state encoded in polarization into spatial split of M output slots designed by the metasurface [83].

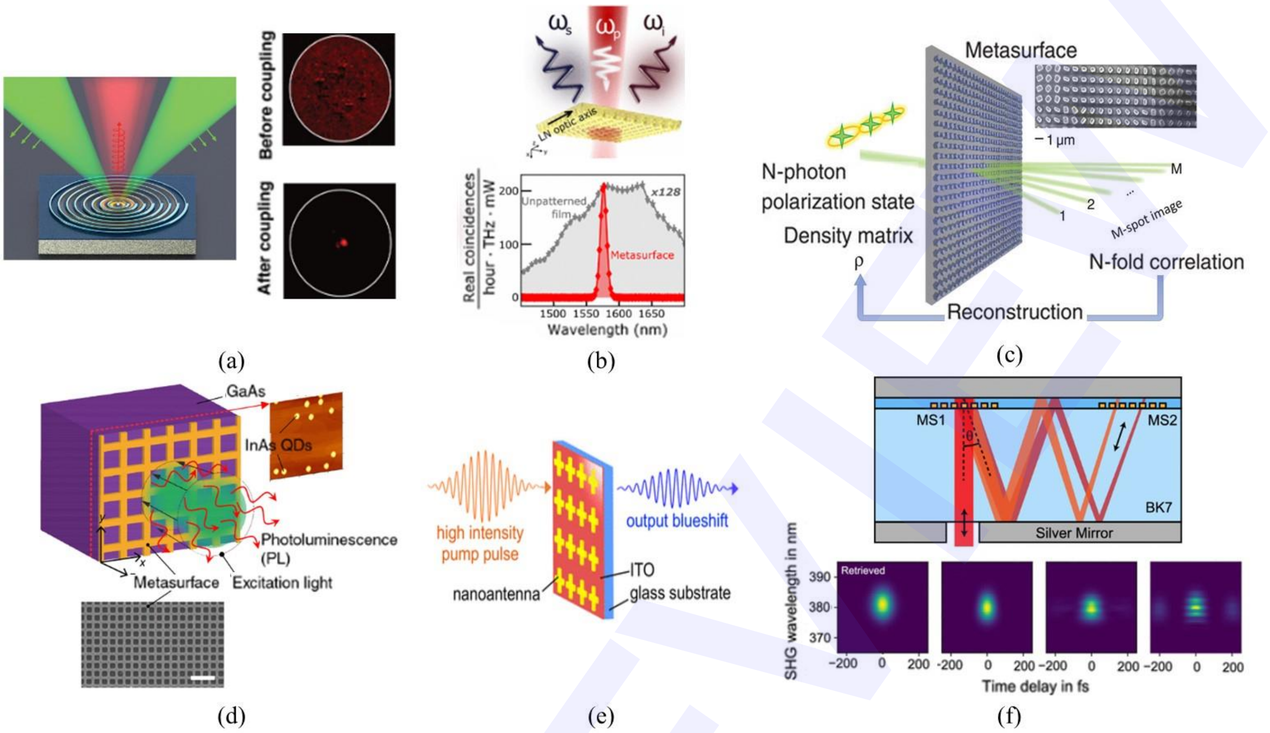

FIG. 6. Metasurfaces for single-photon manipulations and pulse reshaping. (a) Generation of spin angular momentum coded single photon with metasurface. (b) Generation of photon pairs via spontaneous parametric-down conversion in lithium niobate quantum optical metasurfaces. (c) Metasurface for quantum optical state reconstruction. (d) Observation of photoluminescence dynamics in plasmonic metasurface coupled with quantum dots. (e) Using epsilon-near-zero metasurface for photon acceleration. (f) Compact optical pulse shaping device consists of two metasurfaces within parallel silver mirrors. Reprinted with permission from [81], [82], [83], [84], [86] and [87].

In addition to photon manipulations, metasurface has also been used to enhance the photoluminescence (PL), which is a light emission phenomenon from a matter stimulated by another external light energy. As shown in Fig. 6(d), configuration to couple plasmonic metasurfaces with a layer of quantum dots (QDs) has been demonstrated to enhance the PL intensity [84]. Here, it has shown that the Ag nano mesh structure of 330 nm periodicity, optimized by rigorous coupled-wave analysis of scattering-matrix algorithm, is fabricated on the InAs QDs. High absorption of light from the metasurface may lead to the fluorescence enhancement.

Another extraordinary flat optical functionality observed through the metasurface is a photon acceleration from a time-varying epsilon-near-zero metasurface, which is depicted in Fig. 6(e). The photon acceleration, first experimentally observed in the optical domain using gaseous plasma [85], is a kind of nonlinear light phenomenon that indicates the self-driven frequency blueshift of a beam due to the time varying effect induced by the same beam. To achieve such characteristics, the medium itself needs to have time varying characteristics, which is not simply achieved in normal dielectrics, but can be achieved through the epsilon-near-zero metamaterial made by indium tin oxide (ITO) antenna array. The work shown in Fig. 6(e) observe blueshift of the excitation pulse where the amount of blueshift is increased according to the incident intensity [86].

At last, the work shown in Fig. 6(f) demonstrate the application of metasurfaces for reshaping the pulse [87]. The proposed structure consists of two metasurfaces laterally placed along the single side of silver mirror cavity. When incident light illuminates the first metasurface, the first metasurface is designed to have focusing and steering properties simultaneously. Here, the focal point properties are differently designed according to the incident spectra therefore it is focused at the different points at the second metasurface. The second metasurface is designed to spectral encoding with reverse phase gradient respect to the first metasurface, similar to act a retroreflector [88] with spectral encoding. By applying the proposed structure it has been shown that precise spectral tuning of incident pulse can be obtained, by appropriately designing the phase shift profile of the second metasurface.

IV. CONCLUSION

In conclusion, the advancement of metasurface technology has substantially revolutionized optical manipulation, overcoming the limitations of traditional bulk optical components and enabling unprecedented functionalities. Through the effective design of meta-atoms, we have witnessed a range of applications such as wavefront shaping, beam forming, phase gradient design, retroreflection, and single-photon generation and manipulation, etc. The development of metasurfaces also provides a paradigm shift towards flat-optics, characterized by planar, lightweight, and ultra-thin devices, which offer high precision and degree of freedom in designing. As we explore further the electromagnetic and quantum phenomena driven in metasurface, we anticipate the unveiling of novel optical functionalities in flat optics designing. This burgeoning field of metasurfaces promises exciting opportunities for future photonic technologies, bringing us closer to the era of fully integrated and miniaturized optical systems.

FUNDING

This work is supported by the National Research Foundation of Korea funded by the Korea government Ministry of Science and ICT (No. 2022R1F1A1062278) and the Technology Innovation Program (P20019400) funded by the Ministry of Trade, Industry & Energy (MOTIE, Korea)

DISCLOSURES

The authors declare that they have no known competing financial interests or personal relationships that could have appeared to influence the work reported in this paper.

DATA AVAILABILITY

Data sharing is not applicable to this article as no new data were created or analyzed in this study.

REFERENCES

[1] B. Lee, "Review of the present status of optical fiber sensors," Opt. Fiber Technol. **9**(2), 57–79 (2003).

[2] M. Yamaguchi, "Light-field and holographic three-dimensional displays," J. Opt. Soc. Am. A **33**(12), 2348–2364 (2016).

[3] K.-N. Joo and H. M. Park, "Shearing Interferometry: Recent Research Trends and Applications," Curr. Opt. Photon. **7**(4), 325-336 (2023).

[4] S. A. Maier, "Plasmonics: The Promise of Highly Integrated Optical Devices," IEEE. J. Sel. Top. Quant. **12**(6), 1671-1677 (2006).

[5] B. Lee, I.-M. Lee, S. Kim, D.-H. Oh and L. Hesselink, "Review on subwavelength confinement of light with plasmonics," J. Mod. Optics **57**(16), 1479-1497 (2010).

[6] F. Ding, A. Pors and S. I. Bozhevolnyi, "Gradient metasurfaces: a review of fundamentals and applications," Rep. Prog. Phys. **81**(2),

026401 (2017).

[7] S. H. Cha, S. J. Park and Y. H. Ahn, "Investigation of sensitivity distribution in THz metamaterials using surface functionalization," Curr. Opt. Photon., 3 (6), 566-570 (2019).

[8] F. Li, Y. Tang, Q. Peng and G. Hu, "Environment-dependent Broadband Perfect Absorption of Metal-insulator-metal Metamaterial Systems," Curr. Opt. Photon., 7 (2), 136-146 (2023).

[9] H.-C. Ryu "Analysis of the THz Resonance Characteristics of H-shaped Metamaterials with Varying Width," Curr. Opt. Photon., **5** (1), 66-71 (2021).

[10] Y. Li, X. Wang and Y. Zhang, "Dual-function Dynamically Tunable Metamaterial Absorber and Its Sensing Application in the Terahertz Region," Curr. Opt. Photon., 6 (3), 252-259 (2022).

[11] N. Yu and F. Capasso, "Flat optics with designer metasurfaces," Nat. Mater. **13**, 139-150 (2014).

[12] M. Kim, A. M. H. Wong and G. V. Eleftheriades, "Optical Huygens' Metasurfaces with Independent Control of the Magnitude and Phase of the Local Reflection Coefficients," Phys. Rev. X **4**, 041042 (2014).

[13] H.-T. Chen, A. J. Taylor and N. Yu, "A review of metasurfaces: physics and applications," Rep. Prog. Phys. **79**(7)**,** 076401 (2016)**.**

[14] A. Li, S. Singh and D. Sievenpiper, "Metasurfaces and their applications," Nanophotonics **7**(6), 989-1011 (2018).

[15] N. Yu, P. Genevet, M. A. Kats, F. Aieta, J.-P. Tetienne, F. Capasso and Z. Gaburro "Light propagation with phase discontinuities: generalized laws of reflection and refraction," Science **334** (6054), 333-337 (2011).

[16] F. Aieta, P. Genevet, N. Yu, M. A. Kats, Z. Gaburro and F. Capasso, "Out-of-plane reflection and refraction of light by anisotropic optical antenna metasurfaces with phase discontinuities," Nano Lett. **12**(3), 1702-1706 (2012).

[17] L. Liu, X. Zhang, M. Kenney, X. Su, N. Xu, C. Ouyang, Y. Shi, J. Han, W. Zhang and S. Zhang, "Broadband metasurfaces with simultaneous control of phase and amplitude," Adv. Mater. **26**(29), 5031-5036 (2014).

[18] A. Y. Lim and J. W. Lee, "Incident-angle-based Selective Tunability of Resonance Frequency in Terahertz Planar Metamolecules," Curr. Opt. Photon., **6** (6), 590-597 (2022).

[19] S. Sun, K.-Y. Yang, C.-M. Wang, T.-K. Juan, W. T. Chen, C. Y. Liao, Q. He, S. Xiao, W.-T. Kung, G.-Y. Guo, L. Zhou and D. P. Tsai, "High efficiency broadband anomalous reflection by gradient meta-surfaces," Nano Lett. **12**(12), 6223–6229 (2012).

[20] X. Ni, S. Ishii, A. V. Kildishev and V, M. Shalaev, "Ultra-thin, planar, Babinet-inverted plasmonic metalenses," Light Sci. Appl. **2**(4), e72 (2013)

[21] S. Lee and J.-H. Kang, "Babinet-principle-inspired Metasurfaces for Resonant Enhancement of Local Magnetic Fields," Curr. Opt. Photon., **7** (1), 97-103 (2023).

[22] H. Kim and S.-Y. Lee, "Optical Phase Properties of Small Numbers of Nanoslits and an Application for Higher-efficiency Fresnel Zone Plates," Curr. Opt. Photon., 3(4), 285-291 (2019).

[23] Y. F. Yu, A. Y. Zhu, R. Paniagua-Domínguez, Y. H. Fu, B. Lukyanchuk and A. I. Kuznetsov, "High-transmission dielectric metasurface with 2π phase control at visible wavelengths," Laser Photonics Rev. **9**(4), 412-418 (2015).

[24] Q. Zheng, Y. Li, J. Zhang, H. Ma, J. Wang, Y. Pang, Y. Han, S. Sui, Y. Shen, H. Chen and S. Qu, "Wideband, wide-angle coding phase gradient metasurfaces based on Pancharatnam-Berry phase," Sci. Rep. **7**, 43543 (2017).

[25] J.-S. Li and J.-Q. Yao, "Manipulation of terahertz wave using coding Pancharatnam–Berry phase metasurface," IEEE. Photonics J. **10**(5), 1-12 (2018).

[26] M. Khorasaninejad, W. T. Chen, R. C. Devlin, J. Oh, A. Y. Zhu and Federico Capasso, "Metalenses at visible wavelengths: Diffraction-limited focusing and subwavelength resolution imaging," Science **352**(6290), 1190-1194 (2016).

[27] J. Zeng, L. Li, X. Yang and J. Gao, "Generating and separating twisted light by gradient−rotation split-ring antenna metasurfaces," Nano Lett. **16**(5), 3101-3108 (2016).

[28] D. Wen, F. Yue, G. Li, G. Zheng, K. Chan, S. Chen, M. Chen, K. F. Li, P. W. H. Wong, K. W. Cheah, E. Y. B. Pun, S. Zhang and X. Chen, "Helicity multiplexed broadband metasurface holograms," Nat. commun. **6,** 8241 (2015).

[29] G. Zheng, H. Mühlenbernd, M. Kenney, G. Li, T. Zentgraf and S.

Zhang, “Metasurface holograms reaching 80% efficiency,” Nat. Nanotechnol. **10**, 308-312 (2015)

[30] M. Khorasaninejad, A. Y. Zhu, C. Roques-Carmes, W. T. Chen, J. Oh, I. Mishra, R. C. Devlin and F. Capasso, “Polarization-Insensitive Metalenses at Visible Wavelengths,” Nano Lett. **16**(11), 7229-7234 (2016).

[31] Z.-B. Fan, Z.-K. Shao, M.-Y. Xie, X.-N. Pang, W.-S. Ruan, F.-L. Zhao, Y.-J. Chen, S.-Y. Yu and J.-W. Dong, “Silicon Nitride Metalenses for Close-to-One Numerical Aperture and Wide-Angle Visible Imaging,” Phys. Rev. Applied **10**, 014005 (2018).

[32] E. Arbabi, A. Arbabi, S. M. Kamali, Y. Horie and A. Faraon, "Multiwavelength metasurfaces through spatial multiplexing," Sci. Rep., **6**, 32803 (2016).

[33] R. Fu, X. Shan, L. Deng, Q. Dai, Z. Guan, Z. Li, and G. Zheng, "Multiplexing meta-hologram with separate control of amplitude and phase," Opt. Express, **29** (17), 27696-27707 (2021).

[34] D. Wen, F. Yue, S. Kumar, Y. Ma, M. Chen, X. Ren, P. E. Kremer, B. D. Gerardot, M. R. Taghizadeh, G. S. Buller and X. Chen "Metasurface for characterization of the polarization state of light," Opt. Express, **23** (8), 10272-10281 (2015).

[35] L. Deng, Z. Li, Z. Guan, J. Tao, G. Li, X. Zhu, Q. Dai, R. Fu, Z. Zhou, Y. Yang, S. Yu, G. Zheng, "Full Complex-Amplitude Engineering by Orientation-Assisted Bilayer Metasurfaces," Adv. Opt. Mater., **11** (9), 2203095 (2023).

[36] W. Wan, J. Gao and X. Yang, "Full-Color Plasmonic Metasurface Holograms," ACS Nano, **10** (12), 10671–10680 (2016).

[37] S.-Y. Lee, Y.-H. Kim, S.-M. Cho, G. H. Kim, T.-Y. Kim, H. Ryu, H. N. Kim, H. B. Kang, C.-Y. Hwang, and C.-S. Hwang, "Holographic image generation with a thin-film resonance caused by chalcogenide phase-change material," Sci. Rep. **7**, 41152 (2017).

[38] C.-Y. Hwang, G. H. Kim, J.-H. Yang, C.-S. Hwang, S.M. Cho, W.-J. Lee, J.-E. Pi, J.H. Choi, K. Choi, H.-O. Kim, S.-Y. Lee, and Y.-H. Kim, “Rewritable full-color computer-generated holograms based on color-selective diffractive optical components including phase-change materials,” Nanoscale **10**, 21648-21655 (2018).

[39] Y. Hu, X. Luo, Y. Chen, Q. Liu, X. Li, Y. Wang, N. Liu and H. Duan, “3D-Integrated metasurfaces for full-colour holography,” Light Sci. Appl. **8**, 86 (2019).

[40] H. Gao, Y. Wang, X. Fan, B. Jiao, T. Li, C. Shang, C. Zeng, L. Deng, W. Xiong, J. Xia and M. Hong, “Dynamic 3d meta-holography in visible range with large frame number and high frame rate,” Sci. Adv. **6**(28), eaba8595 (2020).

[41] W.-J. Joo, J. Kyoung, M. Esfandyarpour, S.-H. Lee, H. Koo, S. Song, Y.-N. Kwon, S. H. Song, J. C. Bae, A. Jo, M.-J. Kwon, S. H. Han, S.-H. Kim, S. Hwang, M. L. Brongersma, “Metasurface-driven OLED displays beyond 10,000 pixels per inch,” Science **370** (6515), 459-463 (2020).

[42] X. Zou, Y. Zhang, R. Lin, G. Gong, S. Wang, S. Zhu and Z. Wang, “Pixel-level bayer-type colour router based on metasurfaces,” Nat. Commun. **13**, 3288 (2022).

[43] G.-Y. Lee, J.-Y. Hong, S. Hwang, S. Moon, H. Kang, S. Jeon, H. Kim, J.-H. Jeong, and B. Lee, "Metasurface eyepiece for augmented reality," Nat. Commun. **9**, 4562 (2018).

[44] M. Pan, Y. Fu, M. Zheng, H. Chen, Y. Zang, H. Duan, Q. Li, M. Qiu and Y. Hu, “Dielectric metalens for miniaturized imaging systems: progress and challenges,” Light Sci. Appl. **11**, 195 (2022).

[45] W. Feng, J. Zhang, Q. Wu, A. Martins, Q. Sun, Z. Liu, Y. Long, E. R. Martins, J. Li and H. Liang, “RGB Achromatic metalens doublet for digital imaging,” Nano Lett., **22** (10), 3969-3975 (2022).

[46] J. Yang, Z. Zhou and Z. Song, "Broadband plasmonic metasurface for spin-selective hologram in near-infrared band," J. Appl. Phys., 134 (4), 043101 (2023).

[47] Q. Deng, J. Yang, X. Lan, W. Zhang, H. Cui, Z. Xie, L. Li and Y. Huang, "Investigations of generalized Pancharatnam-Berry phase in all-dielectric metasurfaces," Results Phys., 51, 106730 (2023).

[48] X. Liu, Z. Yan, E. Wang, X. Zhao, T. Zhang and F. Fan, "Bifunctional Full-Space Metasurface Combining Pancharatnam–Berry and Propagation Phases," IEEE Antennas Wirel. Propag. Lett., 21 (10), 2110-2114, (2022).

[49] M. Liu, W. Zhu, P. Huo, L. Feng, M. Song, C. Zhang, L. Chen, H. J. Lezec, Y. Lu, A. Agrawal and T. Xu, "Multifunctional metasurfaces enabled by simultaneous and independent control of phase and amplitude for orthogonal polarization states," Light Sci. Appl. 10, 107 (2021).

[50] X. Wang, J. Wu, R. Wang, L. Li and Y. Jiang, "Reconstructing Polarization Multiplexing Terahertz Holographic Images with Transmissive Metasurface," Appl. Sci., 13(4), 2528 (2023).

[51] R. Zhao, G. Geng, Q. Wei, Y. Liu, H. Zhou, X. Zhang, C. He, X. Li, X. Li, Y. Wang, J. Li and L. Huang, "Controllable Polarization and Diffraction Modulated Multi-Functionality Based on Metasurface," Adv. Optical Mater., 10, 2102596 (2022).

[52] X. Ou, T. Zeng, Y. Zhang, Y. Jiang, Z. Gong, F. Fan, H. Jia, H. Duan and Y. Hu, "Tunable Polarization-Multiplexed Achromatic Dielectric Metalens," Nano Lett., **22** (24), 10049–10056 (2022).

[53] J. Wu, Z. Shen, S. Ge, B. Chen, Z. Shen, T. Wang, C. Zhang, W. Hu, K. Fan, W. Padilla, Y. Lu, B. Jin, J. Chen and P. Wu "Liquid crystal programmable metasurface for terahertz beam steering," Appl. Phys. Lett., **116** (13), 131104 (2020).

[54] H. Ren, X. Fang, J. Jang, J. Bürger, J. Rho and S. A. Maier, "Complex-amplitude metasurface-based orbital angular momentum holography in momentum space," Nat. Nanotechnol., **15**, 948-955 (2020).

[55] J. Kim, D. Jeon, J. Seong, T. Badloe, N. Jeon, G. Kim, J. Kim, S. Baek, J.-L. Lee, and J. Rho, "Photonic encryption platform via dual-band vectorial metaholorams in the ultraviolet and visible," ACS Nano, **16** (3), 3546-3553 (2022).

[56] Q. Wei, L. Huang, R. Zhao, G. Geng, J. Li, X. Li, Y. Wang, "Rotational multiplexing method based on cascaded metasurface holography," Adv. Opt. Mater., **10** (8), 2102166 (2022).

[57] G. Rui, C. Ding, B. Gu, Q. Gan, Q. Zhan and Y. Cui, "Symmetric $Ge_2Sb_2Te_5$ based metamaterial absorber induced dynamic wide-gamut structural color," J. Opt., **22** (8), 085003 (2020).

[58] B. Gholipour, A. Karvounis, J. Yin, C. Soci, K. F. MacDonald and N. I. Zheludev, "Phase-change-driven dielectric-plasmonic transitions in chalcogenide metasurfaces," NPG Asia Mater., **10**, 533–539 (2018).

[59] J. Kyoung, "A Theoretical Study on the Low Transition Temperature of VO_2 Metamaterials in the THz Regime," Curr. Opt. Photon., **6** (6), 583-589 (2022).

[60] S.-J. Kim, "Broadband Phase-change Metagrating Design for Efficient Active Reflection Steering," Curr. Opt. Photon., **5** (2), 134-140 (2021).

[61] C. Choi, S.-E. Mun, J. Sung, K. Choi, S.-Y. Lee and B. Lee, "Hybrid state engineering of phase-change metasurface for all-optical cryptography," Adv. Funct. Mater., **31**, 2007210 (2021).

[62] Y. Shi, C. Wan, C. Dai, Z. Wang, S. Wan, G. Zheng, S. Zhang and Z. Li, "Augmented reality enabled by on-chip meta-holography multiplexing," Laser Photonics Rev., **16** (6), 2100638 (2022).

[63] Z. Li, C. Chen, Z. Guan, J. Tao, S. Chang, Q. Dai, Y. Xiao, Y. Cui, Y. Wang, S. Yu, G. Zheng and S. Zhang, "Three-channel metasurfaces for simultaneous meta-holography and meta-nanoprinting : a single-cell design approach," Laser Photonics Rev., **14** (6), 2000032 (2020).

[64] G. T. England, C. Russell, E. Shirman, T. Kay, N. Vogel and J. Aizenberg, "The Optical Janus Effect: Asymmetric Structural Color Reflection Materials," Adv. Mater., **29** (29), 1606876.

[65] T. Kim, E.-S. Yu, Y.-G. Bae, J. Lee, I. S. Kim, S. Chung, S.-Y. Lee and Y.-S. Ryu "Asymmetric optical camouflage: tuneable reflective colour accompanied by the optical Janus effect," Light Sci. Appl., **9**, 175 (2020).

[66] Y. Lim, I. C. Seo, and Y. C. Jun, "Polarization Distortion and Compensation of Circularly Polarized Emission from Chiral Metasurfaces," Curr. Opt. Photon., **7** (2), 147-156 (2023).

[67] K. Chen, G. Ding, G. Hu, Z. Jin, J. Zhao, Y. Feng, T. Jiang, A. Alù and C.-W. Qiu, "Directional Janus metasurface," Adv. Mater., **32** (2), 1906352 (2020).

[68] R. Ji, C. Jin, K. Song, S.-W. Wang and X. Zhao, "Design of multifunctional Janus metasurface based on subwavelength grating," Nanomaterials, **11** (4), 1034 (2021).

[69] B. Chen, S. Yang, J. Chen, J. Wu, K. Chen, W. Li, Y. Tan, Z. Wang, H. Qiu, K. Fan, C. Zhang, H. Wang, Y. Feng, Y. He, B. Jin, X. Wu, J. Chen and P. Wu, "Directional terahertz holography with thermally active Janus metasurface," Light Sci. Appl. **12**, 136 (2023).

[70] X. Liang, L. Deng, X. Shan, Z. Li, Z. Zhou, Z. Guan and G. Zheng, "Asymmetric hologram with a single-size nanostructured metasurface," Opt. Express **29** (13), 19964-19974 (2021).

[71] H.-D. Jeong, S.-W. Moon and S.-Y. Lee, "Asymmetric Diffraction

in Plasmonic Meta-Gratings Using an IT-Shaped Nanoslit Array," Sensors **21** (12), 4097 (2021).

[72] H.-D. Jeong and S.-Y. Lee, "Metasurface for polarization-independent asymmetric transmission of diffraction property using mixed cavity-aperture array," Optik **274**, 170499 (2023).

[73] T. T. Tran, D. Wang, Z.-Q. Xu, A. Yang, M. Toth, T. W. Odom and I. Aharonovich, "Deterministic Coupling of Quantum Emitters in 2D Materials to Plasmonic Nanocavity Arrays," Nano Lett. 17 (4), 2634-2639 (2017).

[74] Y.-Y. Xie, P.-N. Ni, Q.-H. Wang, Q. Kan, G. Briere, P.-P. Chen, Z.-Z. Zhao, A. Delga, H.-R. Ren, H.-D. Chen, C. Xu and P. Genevet, "Metasurface-integrated vertical cavity surface-emitting lasers for programmable directional lasing emissions," Nat. Nanotechnol. 15, 125–130 (2020).

[75] S. K. H. Andersen, S. Kumar and S. I. Bozhevolnyi, "Ultrabright Linearly Polarized Photon Generation from a Nitrogen Vacancy Center in a Nanocube Dimer Antenna," Nano Lett., 17 (6), 3889–3895 (2017).

[76] Y. Kan and S. I. Bozhevolnyi, "Molding Photon Emission with Hybrid Plasmon-Emitter Coupled Metasurfaces," Adv. Optical Mater.,10, 2102697 (2022).

[77] H. Kim, J. Park, S.-W. Cho, S.-Y. Lee, M. Kang, and B. Lee, "Synthesis and dynamic switching of surface plasmon vortices with plasmonic vortex lens," Nano Lett. **10** (2), 529-536 (2010).

[78] S.-W. Cho, J. Park, S.-Y. Lee, H. Kim, and B. Lee, "Coupling of spin and angular momentum of light in plasmonic vortex," Opt. Express **20** (9), 10083-10094 (2012).

[79] S.-W. Moon, H.-D. Jeong, S. Lee, B. Lee, Y.-S. Ryu and S.-Y. Lee, "Compensation of spin-orbit interaction using the geometric phase of distributed nanoslits for polarization-independent plasmonic vortex generation," Opt. Express **27** (14), 19119-19129 (2019).

[80] Y. Bai, J. Yan, H. Lv and Y. Yang, "Plasmonic vortices: a review," J. Opt. **24**, 084004 (2022).

[81] Y. Kan, S. K. H. Andersen, F. Ding, S. Kumar, C. Zhao, S. I. Bozhevolnyi, "Metasurface-enabled generation of circularly polarized single photons," Adv. Mater. **32** (16), 1907832 (2020).

[82] T. Santiago-Cruz, A. Fedotova, V. Sultanov, M. A. Weissflog, D. Arslan, M. Younesi, T. Pertsch, I. Staude, F. Setzpfandt and M. Chekhova, "Photon pairs from resonant metasurfaces," Nano Lett. **21** (10), 4423–4429 (2021).

[83] K. Wang, J. G. Titchener, S. S. Kruk, L. Xu, H.-P. Chung, M. Parry, I. I. Kravchenko, Y.-H. Chen, A. S. Solntsev, Y. S. Kivshar, D. N. Neshev and A. A. Sukhorukov, "Quantum metasurface for multiphoton interference and state reconstruction," Science, **361** (6407), 1104-1108 (2018).

[84] M. Iwanaga, T. Mano and N. Ikeda, "Superlinear photoluminescence dynamics in plasmon-quantum-dot coupling systems," ACS Photonics, **5** (3), 897-906 (2018).

[85] S. C. Wilks, J. M. Dawson, W. B. Mori, T. Katsouleas and M. E. Jones, "Photon accelerator," Phys. Rev. Lett., **62** (22), 2600-2603 (1989).

[86] C. Liu, M. Z. Alam, K. Pang, K. Manukyan, O. Reshef, Y. Zhou, S. Choudhary, J. Patrow, A. Pennathurs, H. Song, Z. Zhao, R. Zhang, F. Alishahi, A. Fallahpour, Y. Cao, A. Almaiman, J. M. Dawlaty, M. Tur, R. W. Boyd and A. E. Willner, "Photon Acceleration Using a Time-Varying Epsilon-near-Zero Metasurface," ACS Photonics, **8** (3), 716-720 (2021).

[87] R. Geromel, P. Georgi, M. Protte, S. Lei, T. Bartley, L. Huang and T. Zentgraf, "Compact metasurface-based optical pulse-shaping device," Nano Lett., **23**, 3196-3201 (2023).

[88] A. Arbabi, E. Arbabi, Y. Horie, S. M. Kamali and A. Faraon, "Planar metasurface retroreflector," Nat. Photonics, **11**, 415-420 (2017).